European Radiology (2018) 28:3760–3769
https://doi.org/10.1007/s00330-018-5352-z

UROGENITAL

Multiparametric MRI for Suspected Recurrent Prostate Cancer after HIFU: Is DCE still needed?

Raïssa Lotte[1] · Alexandre Lafourcade[2] · Pierre Mozer[3] · Pierre Conort[3] · Eric Barret[4] · Eva Comperat[5] · Malek Ezziane[1] · Paul-Hugo Jouve de Guibert[1] · Sebastian Tavolaro[6] · Lisa Belin[2] · Franck Boudghene[6] · Olivier Lucidarme[1] · Raphaële Renard-Penna[1,6,7]

Received: 27 December 2017 / Accepted: 23 January 2018 / Published online: 9 April 2018

Abstract

Purpose To assess the added value of the dynamic contrast-enhanced sequence (DCE) to combination T2-weighted imaging (T2w) + diffusion-weighted imaging (DWI) in detecting prostate cancer (PCa) recurrence after HIFU (high-intensity focused ultrasound).

Methods Forty-five males with clinical and biological suspected PCa recurrence were retrospectively selected. All underwent multi-parametric MRI (mpMRI) before biopsies. Two readers independently assigned a Likert score of cancer likelihood on T2w + DWI + DCE and T2w + DWI images. Prostatic biopsies were taken as the gold standard.

Results Recurrent PCa was identified at biopsy for 37 patients (82%). Areas under the receiver-operating curve of T2w + DWI and T2w + DWI + DCE imaging were not significantly different for both readers. Using a Likert score ≥ 3 for the PCa diagnosis threshold, sensitivity at the lobe level for the (1) senior and (2) junior reader for T2w +DWI +DCE sensitivity was (1) 0.97 and (2) 0.94 vs. (1) 0.94 and (2) 0.97 for T2w + DWI.

Conclusion Accuracy of mpMRI was not significantly improved by adding DCE to T2w + DWI. Sensitivity was high for T2w + DWI + DCE and T2w + DWI with no significant difference for either the junior or senior reader.

Key Points

- *MpMRI has the capability to detect PCa recurrence in post-HIFU monitoring.*
- *The sensitivity of T2w and DWI for detecting PCa recurrence was not improved by DCE.*
- *Readers with different degrees of experience did not improve their performance with DCE.*

Keywords Prostate cancer · Neoplasm recurrence, local · High-intensity focused ultrasound ablation · Diffusion magnetic resonance imaging · Contrast media

Electronic supplementary material The online version of this article (https://doi.org/10.1007/s00330-018-5352-z) contains supplementary material, which is available to authorized users.

✉ Raïssa Lotte
raissalotte@hotmail.com

✉ Raphaële Renard-Penna
raphaele.renardpenna@gmail.com

[1] Academic Department of Radiology, Hopital Pitié-Salpétrière, AP-HP, Sorbonne University, Paris, France

[2] Academic Department of Statistic, Hopital Pitié-Salpétrière, AP-HP, Sorbonne University, Paris, France

[3] Academic Department of Urology, Hopital Pitié-Salpétrière, AP-HP, Sorbonne University, Paris, France

[4] Urology Department, Montsouris Institute, F-75014 Paris, France

[5] Academic Department of Pathology, Hopital Pitié-Salpétrière, AP-HP, Sorbonne University, Paris, France

[6] Academic Department of Radiology, Hopital Tenon, AP-HP, Sorbonne University, Paris, France

[7] GRC5, ONCOTYPE-Uro, Institut Universitaire de Cancérologie, F-75020 Paris, France

Abbreviations

3D	3-dimensional
ADC	Apparent diffusion coefficient
AS	Anterior fibromuscular stroma
AUROC	Area under the ROC curve
CSC	Confidential interval
CI	Clinically significant cancer
DCE	Dynamic contrast enhancement sequence
Dw	Diffusion- weighted imaging
ERBT	External beam radiation therapy
HIFU	High-intensity focused ultrasound
IQR	Interquartile range
mpMRI	Multiparametric magnetic resonance imaging
MRI	Magnetic resonance imaging
PCa	Prostate cancer
PSA	Prostate-specific antigen
ROI	Region of interest
ROC	Receiver-operating characteristic
Se	Sensitivity
Sp	Specificity
STB	Standard biopsy
T2w	T2-weighted imaging
TB	Targeted biopsies
TRUS	Trans-rectal ultrasound

Introduction

Focal treatments of prostate cancer (PCa) are expected to become a standard option for selected patients [1], trying to limit the side effects of radical treatment such as surgery or external beam radiation therapy (ERBT). Among them, high-intensity focused ultrasound (HIFU) ablation has been the most evaluated since the early 1990s [2]. HIFU is a therapeutic option for patients of advanced age, at low-to-intermediate risk, with a low rate of serious side effects [3]. However, one of the principal concerns in focal therapy is the lack of a validated, noninvasive test for monitoring oncological outcome. Although prostate-specific antigen (PSA) is an established monitoring tool after radical treatment [4], its value after focal treatment is uncertain because of the contribution of the residual prostate. Because biopsy is an invasive procedure with significant morbidity [5], exposed to inaccurate sampling and undergrading [6], the MRI-transrectal ultrasound (TRUS) fusion system with target biopsies is now considered best for the follow-up of focal therapy [7]. MpMRI has the capability to monitor the whole prostate (treated and untreated) and to provide information on changes in characteristics that might suggest residual or recurrent disease. Few studies have evaluated mpMRI for HIFU monitoring [8–11]. DCE has shown encouraging results for the detection of local recurrence after HIFU [8]. DWI has not been evaluated in this situation to the best of our knowledge. Based on continuous improvement of DWI [12], and recent concerns about repeated injection of gadolinium chelates [13–15], our aim was to evaluate the added value of DCE to the combination of T2w and DWI for the detection of PCa recurrences after HIFU, using prostate biopsy as a reference standard.

Patients and methods

Institutional Review Board

The creation of the database comprising mpMRI examinations and corresponding pathological data was declared to the appropriate administrative authority. At our institution, all patients undergoing prostate mpMRI with subsequent biopsy give written consent for the use of their MR and pathological data for research purposes. Every patient signed an informed consent form agreeing to HIFU therapy and follow-up.

Patients

Between 2012 and 2017, all patients who had MRI and consecutive prostate biopsies for long-term post-HIFU surveillance were selected from our prospective database. A search was performed to identify patients who fulfilled the inclusion criteria: (1) histologically proven PCa treated with HIFU (focal or partial HIFU), (2) available post-treatment mpMRI of the prostate, including T2w, DWI (b-value up to 1400 or 2000 s/mm^2) and DCE sequences, (3) available post-treatment TRUS-guided biopsy following the mpMRI within 3 months. HIFU treatment was offered to patients with clinically localised PCa who either were assessed to be unsuitable for surgery (e.g. because of advanced age or comorbidity) or declined radical treatment after informed consent. The patients could be classified as low or intermediate risk according to D'Amico's 2003 [16] risk group categories: T1c, T2a, PSA less than 10 ng/ml, and with a Gleason grade of 6 (3+3) or 7 (3+4, or 4 +3). For the patients with Gleason 6 PCa, treatment was decided in accordance with the patient's willingness to be treated after receiving information on the procedure and outcomes [17, 18]. These patients had undergone no prior treatment for PCa.

HIFU procedure

All patients underwent HIFU focal or hemi-ablation under transrectal ultrasound guidance using the Ablatherm ® Integrated Imaging™ (Vaulx-en-Velin, France) device. If necessary, a trans-urethral resection was performed before ablation.

Table 1. ESUR recommendation-compliant description of multiparametric MRI protocol

	1.5-T MRI					3-T MRI	
	T2-weighted BLADE axial sequence	T2-weighted BLADE sagittal sequence	DW imaging	VIBE dynamic contrast -enhanced imaging	T2-weighted 3D	DW Imaging	VIBE dynamic contrast -enhanced imaging
Section thickness/gap (mm)	2.5/0.8	3.5/0.4	3/0.6	3	2.5/0.8	3/0.6	3
Phase-encoding direction	Antero-posterior	Antero-posterior	Antero-posterior	Antero-posterior	Antero-posterior	Antero-posterior	Antero-posterior
Repetition time (ms)	3120	3120	3120	3120	3120	3120	3120
Echo time (ms)	127	119	63	2.15	127	63	2.15
Field of view	200 × 200	200 × 200	220 × 220	208 × 210	200 × 200	220 × 220	208 × 210
Acquisition matrix	320 × 320	320 × 320	174 × 260	178 × 224	320 × 320	174 × 260	178 × 224
b Values (s/mm^2)			50, 400, 1400			50, 400, 2000	
No. of repetitions	1	1	4, 7, 13	1	1	4, 7, 13	1
Turbo factor	24	24			24		
Acquisition duration	3 min 45 s	3 min 13 s	5 min	2 min 40 s	3 min 45 s	5 min	2 min 40 s
Flip angle (degrees)	150	150	90	10	150	90	10

The 1.5-T MR imaging unit (Aera; Siemens, Erlangen, Germany) and 3-T MR imaging unit (Skyra; Siemens, Erlangen, Germany) with a 16-channel PPA receive coil. All patients received 1 mg glucagon intravenously. An endorectal coil was not used

MRI procedure

All images were acquired with a 1.5- (n = 27) or 3-T (n = 18) MR imaging system (Aera 1.5T MRI and Skyra 3T MRI, Siemens Healthcare, Erlangen, Germany) using a pelvis phased-array coil with 18 channels. All examinations included non-enhanced thin turbo spin-echo T2-weighted (T2w) anatomical images acquired in two planes (axial and sagittal) on the 1.5-T MRI and a three-dimensional single sequence on the 3-T MRI. Axial DWIs were performed using b-values of 50, 400 and 1400 s/mm^2 on the 1.5-T MRI and 50, 400 and 2000 s/mm^2 on the 3-T MRI with an ADC map. DCE was obtained using a fat-saturated T1-weighted fast-field gradient echo sequence. After acquisition of the T1 relaxation data, consecutive dynamic sequences were acquired after an intravenous bolus injection of 20 ml of gadoterate meglumine (Dotarem, Guerbet, Roissy Charles de Gaulle, France), with a temporal resolution of 13-16 s. T2w, DWI and DCE were available for all patients. The description of mpMRI technical parameters is summarised in Table 1.

Image analysis

MRIs were independently read by two radiologists: a senior dedicated radiologist with > 10 years of experience in prostate MRI (R.R.P.) [19, 20] and a junior radiologist with 6 months of experience in prostate imaging (R.L.). Both readers analysed two different imaging data sets with a 4-week interval. The first set (a) was image analysis based on the combination of T2w, DWI and DCE. Four weeks later, set (b) was analysed based on T2w and DWI. Readers were blinded to clinical, laboratory and histological findings. The prostate was divided into six sextants: the right and left base, mid-gland and apex. For each sextant, in each data set, readers evaluated the peripheral zone and the transition zone of the prostate.

The largest lesion was defined as the "index target lesion" [21] and was assigned a Likert score [22] ranging from 1 to 5 regarding the likelihood of the presence of PCa (1, definitely absent; 2, probably absent; 3, indeterminate; 4, probably present; 5, definitely present). A recurrent tumour was defined as a focal nodular area with (1) low signal intensity on T2w images, (2) restricted diffusion on DWI and ADC maps and high signal intensity at a b value ≥ 1400 s/mm^2 on DWI and (3) rapid asymmetric enhancement on DCE images. Perfusion data were visually assessed with perfusion maps.

Morphological data were collected from a third consensual reading: prostatic volume calculated using the ellipsoid formula [23], size of the index lesion, involvement of treated edges (inferior/anterior/lateral), existence of a suspicious contralateral lesion, extra-prostatic extension, pelvic lymph nodes and bone lesions.

Standard of Reference

All patients underwent TRUS-guided biopsy under local anaesthesia. The biopsy procedure followed mpMRI, which was initially read by the senior radiologist (first set T2w, DWI and DCE) in clinical routine practice. As

Table 2. MpMRI descriptive data

MpMRI features	*n* (%)
Zonal anatomy location	
Peripheral zone	32 (69%)
Transition zone	9 (20%)
Anterior fibromuscular stroma	4 (9%)
Apex-middle-base location	
Apex	19 (42%)
Middle	23 (51%)
Base	3 (7%)
Antero-posterior location	
Anterior	23 (51%)
Posterior	20 (45%)
Anterior and posterior	2 (4%)
Location on edge of the treated area	
Anterior edge	11 (24%)
Posterior edge	0
Inferior edge	17 (38%)
Superior edge	0
Lateral edge	4 (9%)
Controlateral target	7 (16%)
Extra-prostatic extension	5 (11%)
Pelvic and retroperitoneal lymph nodes	0
Pelvic suspicious bone lesion	0

MpMRI features for the index target on the final study population, *n* (%): location on zonal prostatic anatomy, on sextant, on the treated edges, contralateral target, extra-prostatic extension, lymph nodes and bone lesion.

the biopsy was not performed by a single operator, different types of approaches were used: (A) standard biopsies (STB) with two systematic samples by sextant, one medial and one lateral; (B) addition of STB and targeted biopsies (TB) using the MRI TRUS fusion system (Koelis®, Grenoble, France); (C) TB without STB. The UroStation™ implements elastic registration to fuse the MRI and 3D TRUS images and allow for guiding and recording core localisations on the 3DTRUS and MRI images [24].

All biopsies were examined by a senior pathologist (E.C.). Biopsies were not assigned a Gleason score because of HIFU tissue modification [25]. The cores were individually inked with different colours to mark the sites from which they were collected. The cassettes were soaked in vials of Bouin solution for 1 s to fix the colours and then preserved in pots with 10% formalin. For each biopsy region, whether systematic or targeted, localisation per lobe and per sextant, involvement of the treated or the untreated lobe, total number/length of cores, the number/length of malignant cores and the maximal length of the malignant core were recorded. A cancer was considered as a clinically significant cancer (CSC) when the core length was > 3 mm [26–28].

Statistical analysis

Qualitative variables were described by numbers, percentage and quantitative variables by their medians and interquartile range (IQR). Performances of each method of MRI were assessed by providing Se and Sp for each Likert score threshold with their 95% bootstrap confidence interval (CI). ROCs were plotted and AUROCs were calculated with their 95% bootstrap confidence interval. The gold standard was the biopsy result. AUROCs were compared with the paired bootstrap test. Se and Sp were compared with the exact McNemar test. Percentages of discordance (with bootstrap CI) between two readers were evaluated. A $p < 0.05$ was considered significant. Statistical analysis was performed with R version 3.4.0.

Results

Population and flow chart

Forty-five males who fulfilled the inclusion criteria were included in the present study (Fig. 1). The median (interquartile range [IQR]) patient age was 72 (68-77) years; the PSA level at inclusion was 4.4 (3.1-8) ng/ml. The median (IQR) time from HIFU therapy to mpMRI was 599 (438-911) days; the interval between mpMRI and biopsy was 47 (29-84) days.

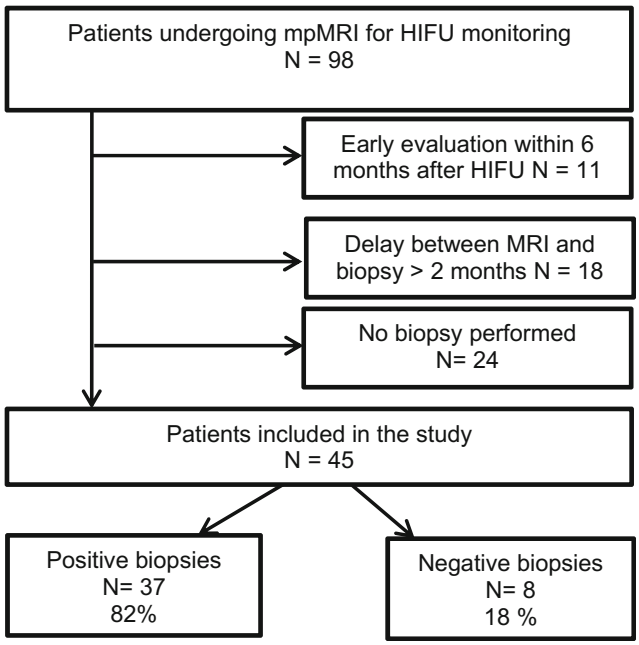

Fig. 1. Flow chart. Exclusion criteria were: post-HIFU procedure early evaluation because of local inflammatory changes (n = 11), no biopsy performed (n = 24) or with a delay > 2 months following the MRI (n = 18) The final study population includes 45 patients.

Table 3. Description of biopsy results

Pathological features	Final population $n = 45$
Biopsy finding, *n* (%)	
(-) Negative	8 (18%)
(+) Untreated lobe	5 (11%)
(+) Treated lobe	29 (64%)
(+) Bilateral	3 (7%)
Clinically significant cancer, *n* (%)	
Treated	20 (44%)
Untreated	1 (2%)
Bilateral	3 (7%)
Localisation, *n* (%)	
Apex	11 (24%)
Apex + middle	6 (13%)
Middle	11 (24%)
Base +middle	11 (24%)
Base	5 (11%)
Apex middle base	1 (3%)

Biopsy results on final study population, *n* (%). No trace of cancer was founded for eight patients (18%). Histological evidence of cancer was found for $n = 37$ patients (82%), in which 24 (54%) had clinically significant cancer. Cancer recurrence at biopsy was mostly located on the treated lobe (64%), with mid-gland involvement (64%), whereas the base was less often involved (11%)

Description of mpMRI target

The median (IQR) prostate volume was 32 (14-35) ml. Targets were located in the peripheral zone (69%), mid-gland (51%) and apex (42%). For 32 patients (71%) targets were located on the treated edge, mostly in the anterior (51%) and inferior part (38%). A contralateral target for the treated area was identified for seven patients (16%). All descriptive mpMRI data are presented in Table 2.

Biopsy findings

Recurrent PCa was identified at biopsy in $n = 37$ (82%) of 45 patients, $n = 24$ (53%) with CSC. The number and localisation of positive biopsies for the final population are summarised in Table 3. Biopsy findings (total and positive respective number/length of cores) are presented for each biopsy procedure group respectively in Table 4. When no lesion was described on MRI, a median of 12 cores was obtained (two systematic samples by sextant, one medial and one lateral) (group A). When a focal lesion was described on MRI, a median of 4.5 targeted cores was obtained (group C) and a median of 14 cores in the group in which both random and targeted biopsies were performed (group B).

The median number of positive cores was 2.5 for a median total of 12 cores (A), 3 for a median total of 14 cores (B) and 1 for a median total of 4.5 cores (C). The median maximal length of positive core was 4 mm for a median total of 111 mm sampled core (A), 20 mm for a median total of 127 mm sampled core (B) and 10 mm for a median total of 45 mm sampled core (C). Among the 33 patients who had STB (A) and STB + TB (B), $n = 21$ patients had positive biopsies in the treated lobe ($n = 6$ patients with non CSC), 3 on the contralateral ($n = 2$ patients with non CSC) and $n = 3$ had bilateral positive biopsies.

Table 4. Respective STB and TB biopsy findings

	(A) STB $n = 19$	(B) STB + TB $n = 14$	(C) TB $n = 12$
Biopsy finding, *n* (%)			
(-) Negative	5 (26%)	1 (7%)	2 (17%)
(+) Untreated lobe	2 (10%)	1 (7%)	0
(+) Treated lobe	12 (63%)	9 (64%)	10 (83%)
(+) Bilateral	0	3 (21%)	0
Clinically significant cancer, *n* (%)			
Treated lobe	5 (26%)	12 (85%)	8 (67%)
Untreated	1 (5%)	3 (25%)	0
Quantitative biopsy results			
Total number of cores, *median (IQR)*	12 (10.5-12)	14 (13.2-14.7)	4.5 (4-5)
Number of positive cores, *median (IQR)*	2.5 (1.2-3.7)	3 (2-4)	1 (1-3)
Total length of cores *mm, median (IQR)*	111 (94.5-133)	127 (81-161)	45 (37.5-62.5)
Length of positive cores, *mm, median (IQR)*	4 (2-16)	20 (3-25)	10 (4-22.2)
Maximal positive core length, *mm, median (IQR)*	3 (2-6)	9 (6-10)	7.5 (4-7.5)

Group A had systematic samples (median number of cores = 12), group B had systematic and targeted sample (median number of cores = 14), and group C had targeted samples only (median number of cores = 4.5). Results suggest that targeted biopsies allowed collecting a better rate of positive core (number and length of positive core) than systematic biopsies alone and a longer malignant length on the core

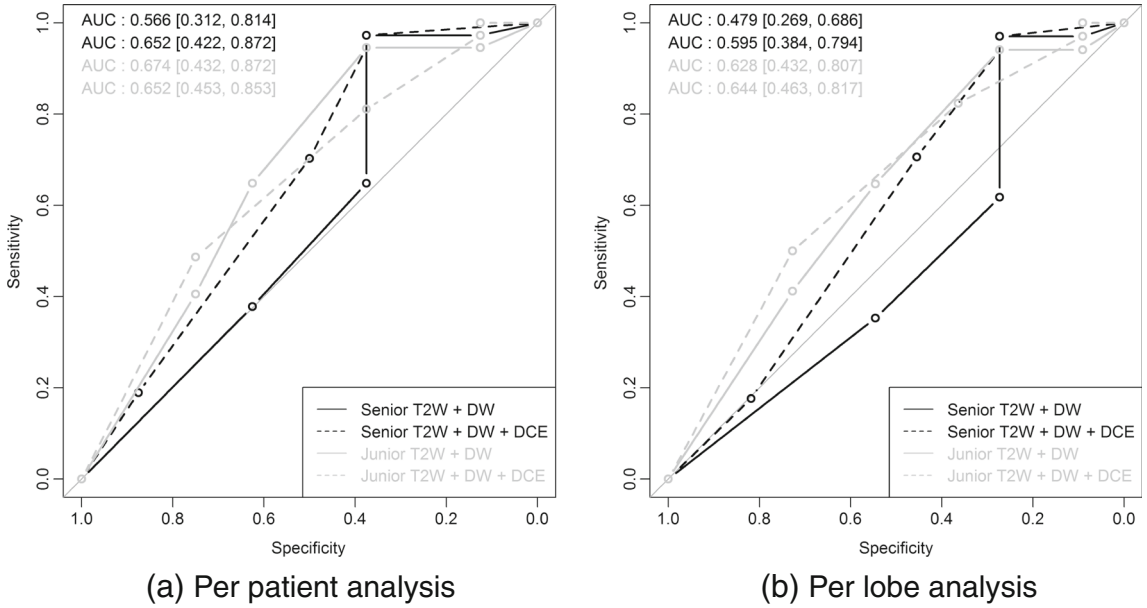

Fig. 2. ROC curves: per-patient analysis (a) and per lobe analysis (b) AUCs were not significantly different between the T2w + DWI and T2w + DWI + DCE combination at (a) the patient level (p values 0.66 for the senior and 0.72 for the junior reader) and (b) the lobe level (p values 0.18 for the senior and 0.78 for the junior reader). Either the junior or senior reader did not improve his diagnostic performance by the addition of DCE

Per-patient analysis

Using a Likert score ≥ of 3/5 for the diagnosis of prostate cancer, sensitivity was not significantly different when evaluating T2w + DWI and T2w + DWI + DCE for diagnosis and was respectively 0.97 [0.91; 1] − 0.95 [0.86; 1] [95 % CI bootstrap] for the senior reader and 0.95 [0.86; 1] − 0.97 [0.92; 1] for the junior reader. For the senior reader the specificity was not significantly different between T2w + DWI and T2w + DWI + DCE and was respectively 0.38 [0; 0.75] − 0.38 [0; 0.75]. For the junior reader the specificity was higher for T2w + DWI: 0.38 [0; 0.73] vs. 0.12 [0; 0.41] for T2w + DW I+ DCE.

For both the senior and junior readers, the AUCs of T2 + DW analysis and T2w + DWI + DCE analysis were not significantly different (p values 0.66 for the senior and 0.72 for the junior reader) (Fig. 2).

Per-lobe analysis

Using a Likert score ≥ 3/5 for the diagnosis of PCa sensitivity was not significantly different for both readers. For T2w + DWI analysis and T2w + DWI + DCE analysis, the sensitivity was respectively 0.97 [0.91; 1] − 0.94 [0.86; 1] [95 CI % bootstrap] for the senior reader and 0.94 [0.84; 1] − 0.97 [0.9; 1] for the junior reader. Specificity for a Likert score ≥ 3 was not different for the senior reader (0.27 [0; 0.57] − 0.27 [0; 0.57]) but was higher for T2w +DWI for the junior reader (0.27 [0; 0.6] − 0.09 [0; 0.29]). Using a Likert score ≥ 4 sensitivity was higher with T2w + DWI + DCE than T2w + DWI for both readers (0. 71 [0.56; 0.86] vs. 0.62 [0.44; 0.79]) for the senior reader, [95 CI % bootstrap] and 0.82 [0.68; 0.94] vs. 0.65 [0.49; 0.79] for the junior reader. Specificity for a Likert score ≥ 4 was higher with T2w + DWI + DCE for the senior reader (0.45 [0.15; 0.78] vs. 0.27 [0; 0.57]) but not for the junior reader (0.36 [0.08; 0.67] vs. 0.55 [0.25; 0.83] − 0.36 [0.08; 0.67]). Results for each Likert group (Likert ≥ 2; Likert ≥ 3; Likert score ≥ 4; Likert = 5) are detailed in Table 5.

For both the senior and junior reader, AUCs of T2 + DW analysis and T2 + DW + DCE analysis were not significantly different (p values 0.18 for the senior and 0.78 for the junior reader) (Fig. 2).

Inter-observer discordance percentage

Inter-observer agreement was not improved by addition of DCE; it was moderate for T2w + DWI analysis (k = 0.54) as well as T2w + DWI + DCE (k = 0.49). For T2 + DW analysis, the discordance percentage between the two readers was 6.7% [0%; 15,6%], with three patients classified in same Likert category (Likert 1 and 2 versus Likert 3, 4 and 5). For T2 + DW + DCE analysis, the discordance percentage between the two readers was 11.1% [2.2%; 22.2%], with five patients classified in same Likert category (Likert 1 and 2 versus Likert 3, 4 and 5) (see details in the supplementary materials).

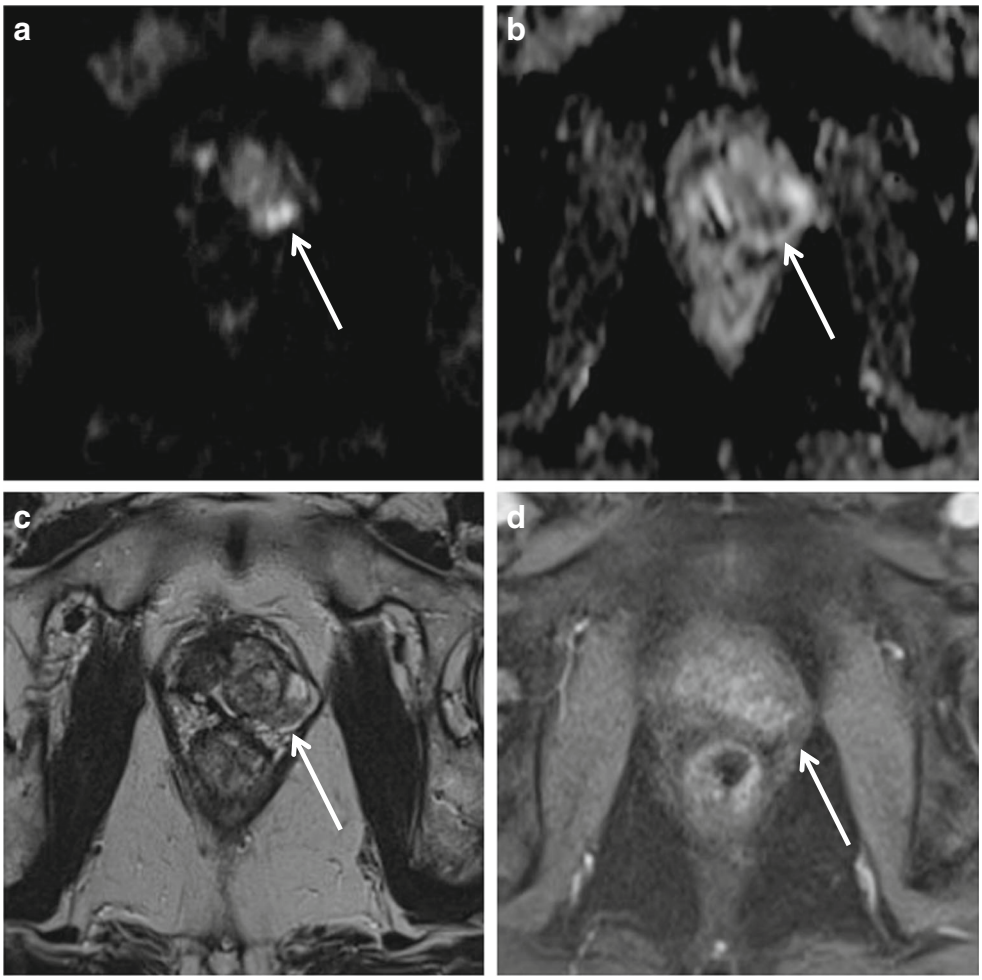

Fig. 3. Case of a 78-year-old patient. Suspicious target on left mid-gland peripheral zone appearing hyperintense on high b-value Dw imaging (a), with low ADC (b), T2w hypointense (c) and ill-defined early enhancement on DCE imaging (d). Among the 12 STB and 2 TB biopsies performed, the presence of PCa was found on two STB cores of the left mid-gland and apical sectors (respectively 4- and-13 mm malignant length) and one left mid-gland TB core (7-mm malignant length)

Discussion

Since the first clinical application of the technique as a single treatment module for locally confined prostate cancer in 1996 [29], high-intensity focused ultrasonic ablation has been widely used in Europe, starting with whole gland ablation and then including hemi- or partial ablation. Detection of local tumour progression after HIFU is important because it can affect decisions about second-line treatment. The significance of PSA is decreasing [3], although the percentage decrease of PSA from before and after focal therapy may have a role in predicting successful ablation of the index lesion [4]. The role of mpMRI in focal therapy for prostate cancer has increased recently but few studies had evaluated MRI techniques for the prediction of local tumour progression in this context [8–11]. To the best of our knowledge, no prior studies have compared the added value of DCE to the combination of T2w + DWI in patients with suspicious local recurrence after focal treatment with HIFU.

In our study we made three important methodological choices. First we evaluated a homogeneous population: patients treated only with focal or hemi-HIFU but not global HIFU, with low-grade disease, advanced age and no prior PCa treatment. All of the patients were referred for long-term monitoring after focal or hemi-HIFU. We excluded immediate post-HIFU evaluation of necrosis and early evaluation usually performed at 3 to 6 month after the treatment. The population was therefore a selected population of patients with available prostatic biopsies following their mpMRI. Our findings can only be considered for those in long-term follow-up after HIFU.

Second, we used a standardised imaging (all patients had an mpMRI with T2w, DWI and DCE imaging) and compared one imaging modality with and without additional information (A vs. A+B). We chose an independent reading design [30, 31]. The reading was split into two different sets with a wash-out delay of 4 weeks at least. Indeed, the interpretation

Table 5. Sensitivity and specificity for Likert ≥ 3 scored mpMRI target [CI 95% bootstrap] for per-patient analysis

Likert score	Se	Sp	TN	FP	FN	TP
Senior T2w + DWI						
≥ 2	0.97 [0.91; 1]	0.09 [0; 0.31]	1	10	1	33
≥ 3	0.97 [0.91; 1]	0.27 [0; 0.57]	3	8	1	33
≥ 4	0.62 [0.44; 0.79]	0.27 [0; 0.57]	3	8	13	21
= 5	0.35 [0.2; 0.52]	0.55 [0.24; 0.83]	6	5	22	12
Senior DCE + T2w + DWI						
≥ 2	0.97 [0.91; 1]	0.27 [0; 0.57]	3	8	1	33
≥ 3	0.94 [0.86; 1]	0.27 [0; 0.57]	3	8	2	32
≥ 4	0.71 [0.56; 0.86]	0.45 [0.15; 0.78]	5	6	10	24
= 5	0.18 [0.06; 0.32]	0.82 [0.56; 1]	9	2	28	6
Junior T2w + DWI						
≥ 2	0.94 [0.84; 1]	0.09 [0; 0.3]	1	10	2	32
≥ 3	0.94 [0.84; 1]	0.27 [0; 0.6]	3	8	2	32
≥ 4	0.65 [0.49; 0.79]	0.55 [0.25; 0.83]	6	5	12	22
= 5	0.41 [0.25; 0.59]	0.73 [0.45; 1]	8	3	20	14
Junior DCE + T2w + DWI						
≥ 2	1 [1; 1]	0.09 [0; 0.29]	1	10	0	34
≥ 3	0.97 [0.9; 1]	0.09 [0; 0.29]	1	10	1	33
≥ 4	0.82 [0.68; 0.94]	0.36 [0.08; 0.67]	4	7	6	28
= 5	0.5 [0.32; 0.67]	0.73 [0.45; 1]	8	3	17	17

Using a Likert ≥ 3 threshold for diagnosis, sensitivity was good and acceptable for detection use in clinical practice, without any benefit of the addition of DCE (non-significant difference for T2w + DWI and T2 + DWI + DCE) for readers with different degrees of experience. Specificity was low, but also not improved by the addition of DCE

of imaging involves a global cognitive approach and each sequence influences the interpretation of the others. Independent readings are more likely to represent the real situation of having only T2w and Dw for the final mpMRI conclusion. The added value of each modality was tested independently for two different readers, a dedicated senior and junior uro-radiologist, to possibly expand findings to experienced and less-experienced radiologists.

Third, we used a Likert scale with different thresholds instead of the PIRADS score, which was designed for naïve prostate glands [22]. The Likert score has been proven to be a significant predictor of malignancy in untreated and treated patients [20, 30, 32].

Like previously published series evaluating radio-recurrent prostate cancer, we found that AUC values obtained with T2w + DWI and T2w + DWI + DCE imaging were not significantly different [30, 33]. However, AUC values only reflect the global performance of the test and sensitivity and specificity trade-offs must also be compared between the two techniques. For diagnosis of PCa recurrence after HIFU, we found that mpMRI showed higher sensitivity for both readers, with a poor specificity. Our concern was the potential impact of omitting DCE imaging. Sensitivity and specificity were not significantly modified by addition of DCE imaging. Using a Likert threshold ≥ 3/5, the performance of the junior reader was similar to that of the senior reader and DCE did not appear to be more beneficial to him [34]. We found a slight improvement of sensitivity with DCE imaging for both readers with a Likert threshold ≥ 4/5. Since post-HIFU mpMRI monitors conservative treatment with the possibility of other additional treatment options (surgery, ERBT, repeated HIFU), reliability in the detection of recurrence with a high sensitivity is needed. Kim et al. [9] found that, for prediction of the local tumour progression of prostate cancer after HIFU, DCE-MRI was more sensitive but less specific than the combination of T2w and DWI. However, the accuracy rates of DCE-MRI and T2-weighted MRI with DWI were similar.

Inter-observer agreement was moderate for both combinations, but was comparable to that of other studies evaluating MRI for the prediction of local prostate cancer recurrence after treatment. There was also no improvement in inter reader-agreement when DCE was used. Kim et al. [9] found kappa values for DCE MRI and T2-weighted MRI respectively of 0.59 and 0.46 for local recurrence after HIFU. For local recurrence after prostate cancer radiation therapy, Donati et al. [35] found 0.55 and 0.49 for T2w + DW and T2w +DW+ DCE imaging respectively. The assessment of tumour detection and localisation and the differentiation of viable tumour from treated tumour are notoriously difficult because of volume reduction, loss of zonal anatomy, and shape and signal

changes caused by local treatment [36, 37]. Moreover, unlike for naïve prostates, it could reflect the lack of standardisation of reliable criteria for MRI prediction of local prostate cancer recurrence after treatment.

The majority of the mpMRI targets were located on the middle and apex (93%) (Table 2), as previously described by Rischmann [38] (67% rate of apical location) and all localised on the lateral, anterior and inferior edge of the treated zone. This result might be due to the apical safety margin defined in the treatment protocol. The residual disease at the anterior part of the treated area could also be explained by the technical limitations of with a penetration depth < 30 mm.

In a previous study published by Rouvière et al. [8] the detection rate of targeted biopsies was better than for random biopsies in a population for the detection of prostate recurrence after HIFU. In our study, targeted biopsies using TRUS-MR fusion were significantly more likely to contain cancer than STB. TBs were able to diagnose more men with a significant PCa and found more CSCs than non-targeted biopsies. Moreover, PCa undiagnosed by targeted biopsies was usually smaller and less significant than those undiagnosed by random biopsies. This strongly supports that prostate MRI may enable a reduction in the number of cores performed during follow-up biopsies by targeting positive areas, or a reduction in the need for post-treatment biopsy if negative, although this latter application remains speculative.

Our study has some limitations. First, it was a retrospective study and our finding needs to be validated on a larger population. Second, the number of patients was small. HIFU is not widespread in many institutions. Biopsy was not available for all the patients who underwent HIFU at our institution, mostly because of refusal to perform biopsy when MRI did not detect signs of recurrence. Third, salvage prostatectomy is technically difficult and carries a high morbidity rate in this population; therefore we could not use prostatectomy specimens as the reference standard. Finally, images were acquired with 1.5- and 3-T systems, which could affect the performance of this post-treatment context so that we may be underestimating the potential performance of modern MRI with very high b values.

These are encouraging preliminary results, showing the possibility to shorten and simplify everyday practice with a T2w + DWI mpMRI protocol, limiting DCE and so the risk and cost of gadolinium chelate injection.

Funding The authors state that this work has not received any funding.

Compliance with ethical standards

Guarantor The scientific guarantor of this publication is Raphaele Renard Penna.

Conflict of interest The authors of this manuscript declare no relationships with any companies, whose products or services may be related to the subject matter of the article.

Statistics and biometry Alexandre Lafourcade and Lisa Belin (Hopital Pitié Salpétrière) kindly provided statistical advice for this manuscript.

Informed consent Written informed consent was obtained from all subjects (patients) in this study.

Ethical approval Institutional Review Board approval was not required because the methodology of the study was retrospective on imaging materials, without any supplementary interventions than routine practice for medical care.

Methodology
- retrospective
- diagnostic or prognostic study
- performed at one institution

References

1. Sartor AO, Hricak H, Wheeler TM et al (2008) Evaluating localized prostate cancer and identifying candidates for focal therapy. Urology 72:S12–S24
2. Valerio M, Ahmed HU, Emberton M et al (2014) The role of focal therapy in the management of localised prostate cancer: a systematic review. Eur Urol 66:732–751
3. Ganzer R, Fritsche H-M, Brandtner A et al (2013) Fourteen-year oncological and functional outcomes of high-intensity focused ultrasound in localized prostate cancer. BJU Int 112:322–329
4. Abdel-Wahab M, Pollack A (2010) Prostate cancer: Defining biochemical failure in patients treated with HIFU. Nat Rev Urol 7:186–187
5. Loeb S, Vellekoop A, Ahmed HU et al (2013) Systematic review of complications of prostate biopsy. Eur Urol 64:876–892
6. Moore CM, Kasivisvanathan V, Eggener S et al (2013) Standards of reporting for MRI-targeted biopsy studies (START) of the prostate: recommendations from an International Working Group. Eur Urol 64:544–552
7. Scheltema MJ, Tay KJ, Postema AW et al (2017) Utilization of multiparametric prostate magnetic resonance imaging in clinical practice and focal therapy: report from a Delphi consensus project. World J Urol 35:695–701
8. Rouvière O, Girouin N, Glas L et al (2010) Prostate cancer transrectal HIFU ablation: detection of local recurrences using T2-weighted and dynamic contrast-enhanced MRI. Eur Radiol 20:48–55
9. Kim CK, Park BK, Lee HM (2009) Prediction of locally recurrent prostate cancer after radiation therapy: incremental value of 3T diffusion-weighted MRI. J Magn Reson Imaging JMRI 29:391–397
10. Punwani S, Emberton M, Walkden M et al (2012) Prostatic cancer surveillance following whole-gland high-intensity focused ultrasound: comparison of MRI and prostate-specific antigen for detection of residual or recurrent disease. Br J Radiol 85:720–728
11. Hoquetis L, Malavaud B, Game X et al (2016) MRI evaluation following partial HIFU therapy for localized prostate cancer: A single-center study. Prog Urol 26:517–523
12. Rouvière O, Dagonneau T, Cros F et al (2017) Diagnostic value and relative weight of sequence-specific magnetic resonance features in

characterizing clinically significant prostate cancers. PLOS ONE 12:e0178901
13. Ramalho J, Ramalho M, Jay M et al (2016) Gadolinium toxicity and treatment. Magn Reson Imaging 34:1394–1398
14. Reeder SB, Gulani V (2016) Gadolinium deposition in the brain: Do we know enough to change practice? Radiology 279:323–326
15. Conte G, Preda L, Cocorocchio E et al (2017) Signal intensity change on unenhanced T1-weighted images in dentate nucleus and globus pallidus after multiple administrations of gadoxetate disodium: an intraindividual comparative study. Eur Radiol. https://doi.org/10.1007/s00330-017-4810-3
16. D'Amico AV, Moul J, Carroll PR et al (2003) Cancer-specific mortality after surgery or radiation for patients with clinically localized prostate cancer managed during the prostate-specific antigen era. J Clin Oncol 21:2163–2172
17. de la Rosette J, Ahmed H, Barentsz J et al (2010) Focal therapy in prostate cancer-report from a consensus panel. J Endourol 24:775–780
18. Rozet F, Bastide C, Beuzeboc P et al (2015) Prise en charge des tumeurs de la prostate à faible risque évolutif. Prog En Urol 25:1–10
19. Renard-Penna R, Rouprêt M, Comperat E et al (2013) Accuracy of high resolution (1.5 tesla) pelvic phased array magnetic resonance imaging (MRI) in staging prostate cancer in candidates for radical prostatectomy: Results from a prospective study. Urol Oncol 31: 448–454
20. Renard-Penna R, Mozer P, Cornud F et al (2015) Prostate imaging reporting and data system and Likert scoring system: multiparametric MR imaging validation study to screen patients for initial biopsy. Radiology 275:458–468
21. Ahmed HU (2009) The index lesion and the origin of prostate cancer. N Engl J Med 361:1704–1706
22. Barentsz JO, Richenberg J, Clements R et al (2012) ESUR prostate MR guidelines 2012. Eur Radiol 22:746–757
23. Haas M, Günzel K, Miller K et al (2017) Is the ellipsoid formula the new standard for 3-Tesla MRI prostate volume calculation without endorectal coil? Urol Int 98:49–53
24. Mozer P, Rouprt M, Le Cossec C et al (2015) First round of targeted biopsies using magnetic resonance imaging/ultrasonography fusion compared with conventional transrectal ultrasonography-guided biopsies for the diagnosis of localised prostate cancer: MRI/TRUS-fusion targeted vs standard TRUS-guided biopsy. BJU Int 115:50–57
25. Billia M, Siddiqui KM, Chan S et al (2016) Assessment of histopathological features of needle biopsy in recurrent prostate cancer following salvage high-intensity focused ultrasound. Can Urol Assoc J J Assoc Urol Can 10:416–422
26. Valerio M, Donaldson I, Emberton M et al (2015) Detection of Clinically Significant Prostate Cancer Using Magnetic Resonance Imaging-Ultrasound Fusion Targeted Biopsy: A Systematic Review. Eur Urol 68:8–19
27. Schoots IG, Roobol MJ, Nieboer D et al (2015) Magnetic resonance imaging-targeted biopsy may enhance the diagnostic accuracy of significant prostate cancer detection compared to standard transrectal ultrasound-guided biopsy: a systematic review and meta-analysis. Eur Urol 68:438–450
28. Donaldson IA, Alonzi R, Barratt D et al (2015) Focal therapy: patients, interventions, and outcomes–a report from a consensus meeting. Eur Urol 67:771–777
29. Gelet A, Chapelon JY, Bouvier R et al (1996) Treatment of prostate cancer with transrectal focused ultrasound: early clinical experience. Eur Urol 29:174–183
30. Alonzo F, Melodelima C, Bratan F et al (2016) Detection of locally radio-recurrent prostate cancer at multiparametric MRI: Can dynamic contrast-enhanced imaging be omitted? Diagn Interv Imaging 97:433–441
31. Schalekamp S, van Ginneken B, Schaefer-Prokop CM, Karssemeijer N (2014) Influence of study design in receiver operating characteristics studies: sequential versus independent reading. J Med Imaging (Bellingham) 1:015501
32. Rosset R, Bratan F, Crouzet S et al (2017) Can pre- and postoperative magnetic resonance imaging predict recurrence-free survival after whole-gland high-intensity focused ablation for prostate cancer? Eur Radiol 27:1768–1775
33. Abd-Alazeez M, Ramachandran N, Dikaios N et al (2015) Multiparametric MRI for detection of radiorecurrent prostate cancer: added value of apparent diffusion coefficient maps and dynamic contrast-enhanced images. Prostate Cancer Prostatic Dis 18:128–136
34. Hausmann D, Aksöz N, von Hardenberg J et al (2017) Prostate cancer detection among readers with different degree of experience using ultra-high b-value diffusion-weighted Imaging: Is a non-contrast protocol sufficient to detect significant cancer? Eur Radiol. https://doi.org/10.1007/s00330-017-5004-8
35. Donati OF, Jung SI, Vargas HA et al (2013) Multiparametric prostate MR imaging with T2-weighted, diffusion-weighted, and dynamic contrast-enhanced sequences: are all pulse sequences necessary to detect locally recurrent prostate cancer after radiation therapy? Radiology 268:440–450
36. Kirkham AP, Emberton M, Hoh IM et al (2008) MR Imaging of Prostate after Treatment with High-Intensity Focused Ultrasound 1. Radiology 246:833–844
37. Vargas HA, Wassberg C, Akin O, Hricak H (2012) MR imaging of treated prostate cancer. Radiology 262:26–42
38. Rischmann P, Gelet A, Riche B et al (2017) Focal High Intensity Focused Ultrasound of Unilateral Localized Prostate Cancer: A Prospective Multicentric Hemiablation Study of 111 Patients. Eur Urol 71:267–273